Scientific Contributions Oil & Gas, Vol. 49. No. 2, June: 219 - 236

SCIENTIFIC CONTRIBUTIONS OIL AND GAS

Testing Center for Oil and Gas
LEMIGAS

Journal Homepage:http://journal.lemigas.esdm.go.id
ISSN: 2089-3361, e-ISSN: 2541-0520

Synthesis of Boehmite Catalyst Using A Natural Soft Template for The Deoxygenation of Waste Cooking Oil Into Biofuel: Effect of Sapindus Rarak Extraction and Process Optimization

Didi Dwi Anggoro[1], Luqman Buchori[1], M. Hasim Muzadi[1], Brilliant Umara Le Monde[1], Tubagus Rayyan Fitra Sinuhaji[1], Sudiyarmanto[2], and Wawan Rustyawan[3]

[1]Chemical Engineering Department, Universitas Diponegoro,
Prof. Jacub Rais St., Semarang, Indonesia.

[2]Research Center for Molecular Chemistry, National Research and Innovation Agency (BRIN),
KST BJ. Habibie, South Tangerang, Indonesia.

[3]Pertamina Technology Innovation, Pertamina,
Bekasi St., East Jakarta, Indonesia.

Corresponding author: Didi Dwi Anggoro (anggorophd@gmail.com)

Manuscript received: February 12th, 2026; Revised: March 19th, 2026
Approved: April 29th, 2026; Available online: June 09th, 2026; Published: June 09th, 2026.

ABSTRACT - The development of environmentally friendly catalysts for converting waste cooking oil (WCO) into renewable energy continues to attract significant attention. In this study, mesoporous boehmite (γ-AlOOH) was synthesized from alumina derived from Lapindo mud, using *Sapindus rarak* extract (SRE) as a natural soft template. The saponins present in SRE play a role in regulating structure, controlling crystal growth, and enhancing porosity during the hydrothermal synthesis process. Characterization results confirmed the formation of orthorhombic γ-AlOOH, with improved physicochemical properties observed as the SRE concentration increased. The catalyst synthesized with 50 wt% SRE exhibited a surface area of 85.72 m²/g and a well-defined mesoporous structure. Nickel was subsequently incorporated into the 50 wt% SRE-derived γ-AlOOH to generate bifunctional catalytic sites, which are essential for the deoxygenation of WCO into biofuel. Process parameter optimization was conducted using response surface methodology (RSM) with a Box–Behnken design. The optimal reaction conditions were identified as 4 hours of reaction time, a temperature of 350°C, and a catalyst concentration of 5 wt%, resulting in a product yield of 78.37%. GC–MS analysis revealed that the products were predominantly composed of C15–C21 hydrocarbons, indicating biofuel formation via decarboxylation, hydrodeoxygenation, and decarbonylation pathways. This study demonstrates that γ-AlOOH synthesized using an SRE-based template is a promising and sustainable catalyst for biofuel production from WCO.

Keywords: boehmite, sapindus rarak, WCO, biofuel, optimization, deoxygenation.

How to cite this article:

Didi Dwi Anggoro, Luqman Buchori, M. Hasim Muzadi, Brilliant Umara Le Monde, Tubagus Rayyan Fitra Sinuhaji, Sudiyarmanto, and Wawan Rustyawan, 2026, Synthesis of Boehmite Catalyst Using A Natural Soft Template for The Deoxygenation of Waste Cooking Oil Into Biofuel: Effect of Sapindus Rarak Extraction and Process Optimization, Scientific Contributions Oil and Gas, 49 (2) pp. 219-236. DOI org/10.29017/scog.v49i2.2074.

INTRODUCTION

Boehmite (γ-AlOOH) is a porous aluminum oxide hydroxide phase that is widely used as a precursor to γ-Al_2O_3 and as a catalyst support due to its mechanical strength, thermal stability, and modifiable surface acid–base properties (Ibrahim et al., 2026; Sun et al., 2025). Boehmite has an orthorhombic crystal structure composed of AlO_6 sheets, with each layer connected by hydrogen bonds, enabling morphology control during synthesis (Spiegel 2018). Boehmite can be synthesized using various methods, including solvothermal (Ameri et al., 2016), hydrothermal (He et al., 2022), sol–gel (Abdollahifar et al., 2018), and precipitation methods (Toledo-Chávez et al., 2016). Among these methods, hydrothermal synthesis is the most commonly used because it provides a high-pressure aqueous environment at relatively moderate temperatures. This condition enhances the solubility and reactivity of precursors, enabling precise control over the crystallinity, phase purity, and particle morphology of the resulting boehmite while consuming less energy than conventional solid-state calcination (Anggoro et al., 2024). In recent years, most studies on boehmite have focused on controlling crystallite size, pore distribution, and surface area, as these properties strongly influence catalytic performance in various applications. Boehmite with organized mesoporosity can exhibit a high surface area of more than 300 m^2/g and good thermal stability, making it suitable for use as a catalyst in renewable energy applications (Banks & Bridgwater 2016).

One strategy for modifying boehmite mesoporosity is surfactant templating, which controls structural growth through self-assembly. Previous studies have shown that templating agents such as CTAB, Pluronic, and F127 can effectively control morphology and improve the dispersibility of boehmite (Li et al., 2020; Liu et al., 2023; Nugraha et al., 2021). However, their synthetic and non-renewable nature remains a limitation. Environmentally friendly biopolymers, such as xanthan gum, have also been investigated for controlling boehmite morphology (Movasati et al., 2024). Nevertheless, their large molecular size, high viscosity, and hydrophilic nature result in weaker surfactant properties than those of amphiphilic surfactants such as CTAB, leading to less precise micelle control. Therefore, Sapindus rarak extract (SRE), which possesses surfactant properties comparable to CTAB while offering the sustainability advantages of a biopolymer, is a promising green templating agent for replacing synthetic surfactants. SRE is rich in saponins, natural amphiphilic compounds that can self-assemble and regulate boehmite pore formation during nucleation and crystal growth (Aziz et al., 2023; Jovita et al., 2024). Saponins function as soft templates that can be removed by calcination, leaving a uniformly distributed mesoporous network (Aziz et al., 2024). This enhanced porosity can improve active-site accessibility and strengthen metal–support interactions.

The use of mesoporous boehmite derived from Lapindo mud as a catalyst support holds significant potential for the oil and gas sector, particularly in supporting the transition toward more sustainable refining processes. Hydroprocessing technologies, such as hydrocracking and hydrodeoxygenation, are widely applied to produce higher-value fuels from crude hydrocarbons. Compared with thermal methods alone, catalytic technology can improve product selectivity because catalyst pore size can be tailored to direct the formation of desired products. Moreover, catalytic processes are

generally considered more cost-effective than non-catalytic processes, which are often associated with high energy inefficiency (Morina & Sidjabat 2022; Ulfiati 2020). The stability and reusability of boehmite supports are critical factors for industrial applications. Preliminary studies suggest that mesoporous boehmite derived from Lapindo mud can maintain its structural integrity under reaction conditions, thereby supporting its long-term economic viability. Boehmite can also be used as a catalyst support in the deoxygenation of waste cooking oil (WCO) into diesel-equivalent hydrocarbons. WCO contains long-chain hydrocarbons with high molecular weights; therefore, a conversion process is required to break down these heavy fractions into lighter compounds comparable to liquid fuels. With the aid of an appropriate catalyst, deoxygenation can serve as an effective method for cleaving long-chain carbon bonds into shorter hydrocarbon chains (Nasution et al., 2022; Setyawan et al., 2018). The deoxygenation process involves hydrodeoxygenation, decarbonylation, and decarboxylation pathways, which are strongly influenced by catalyst surface area, Lewis and Brønsted acid sites, and pore diffusivity within the boehmite catalyst (Dabbawala et al., 2024). Boehmite and its derivatives, particularly γ-Al_2O_3, provide Lewis acid sites originating from unsaturated and undercoordinated Al^{3+} centers, as well as surface hydroxyl groups that contribute to the activation of polar molecules. These properties support the use of boehmite as an acid catalyst or as a support for transition metals, such as Ni, Cu, Co, and Mo, in WCO deoxygenation reactions (Yang et al., 2023).

Given this context, the novelty of this study is twofold. First, it introduces a highly sustainable synthesis route for mesoporous boehmite by utilizing Lapindo mud as a secondary alumina source and SRE as a fully natural green templating agent, thereby replacing toxic synthetic surfactants. Second, this study demonstrates the specific and enhanced effectiveness of the environmentally friendly synthetic boehmite in the catalytic deoxygenation of WCO by considering reaction time, catalyst mass, and reaction temperature. These variables are important to examine because they are closely related to the kinetics, selectivity, and overall efficiency of the catalytic process. Therefore, this study aims to determine the optimal process parameters for converting WCO into biofuel through catalytic deoxygenation. In addition, it evaluates the effect of SRE concentration on the physicochemical properties of the synthesized boehmite and its correlation with catalytic performance in the WCO deoxygenation process.

METHODHOLOGY

Materials

Lapindo mud from Sidoarjo, Indonesia; Sapindus rarak fruit obtained from a traditional market in Yogyakarta, Indonesia; HNO_3 (35%); HCl (35%); ethanol (70%); and WCO collected from a traditional market in Semarang, Indonesia were used in this study. Prior to use, WCO was filtered via gravity filtration using filter paper to remove residual food particles that could interfere with the reaction process. The chemical composition of WCO was analyzed using GC–MS.

Extraction of sapindus rarak fruit

Extraction of Sapindus rarak fruit was carried out using the maceration method (Aziz et al., 2023). The fruits were washed and oven-dried at 80°C for 12 hours, then ground and sieved to a 100 -mesh size. The resulting powder was soaked in 70% ethanol at a ratio of 1:10 (w/v) in a closed container for 24 hours. The mixture was then filtered, and the filtrate was evaporated at 80°C to obtain SRE. It was subsequently dissolved in distilled water to prepare a surfactant feedstock solution at a concentration of 2 mg/L.

Synthesis of boehmite

Lapindo mud, used as the base material for γ-AlOOH synthesis, was processed via reflux extraction following the method reported by Anggoro et al. (2023) to obtain $Al(OH)_3$ solid (Anggoro et al., 2024). The γ-AlOOH synthesis was conducted using a hydrothermal method. The extracted $Al(OH)_3$ was dispersed in distilled water at a ratio of 1:5 (w/v) and stirred at room temperature. SRE (0, 10, 20, and 50%) was then added to the mixture under continuous stirring. The

pH was adjusted to 9 using 2 M NaOH and 2 M HCl, and stirring was continued for 6 hours until a slurry formed. The mixture was then transferred into a Teflon-lined autoclave and subjected to hydrothermal treatment at 190°C for 24 hours. After calcination, the solid γ-AlOOH was separated by filtration, washed with hot distilled water and ethanol, and dried overnight at 110°C.

To enhance catalytic performance, nickel was introduced using $Ni(NO_3)_2 \cdot 6H_2O$. A 5 wt% Ni $(NO_3)_2 \cdot 6H_2O$ solution was prepared in distilled water, followed by the addition of γ-AlOOH. The mixture was stirred at room temperature for 12 hours, then dried and calcined at 550°C for 3 hours.

Catalytic deoxygenation of WCO

The catalytic deoxygenation of WCO to produce biofuel was carried out in a fixed-bed reactor. For preparation, 2–5 wt% of catalyst (relative to the mass of WCO feedstock) was loaded into a column furnace, with fiberglass used as support material inside the reactor column. Prior to the reaction, the system was purged with N_2 gas at a flow rate of 200 mL min^{-1} for several minutes. The WCO was heated using a heating mantle to a temperature range of 330–370°C. The resulting volatile products passed through a condenser and were collected as liquid biofuel in a bottom flask. Products were collected at hourly intervals (1–4 hours). The biofuel yield was calculated using the following Equation 1:

$$\%\, Yield = \frac{mass\ of\ \ liquid\ product}{initial\ mass\ of\ WCO}\ x\ 100\% \qquad (1)$$

Optimization analysis

The optimization study was conducted using Design-Expert software employing a Box–Behnken Design (BBD). The independent variables selected to determine the optimal conditions for the deoxygenation process were reaction time (X_1: 1–4 hours), catalyst loading (X_2: 1–5 wt%), and reaction temperature (X_3: 330–370°C), with percentage yield as the response variable. The experimental design is presented in Table 3. The obtained data were analyzed using Analysis of Variance (ANOVA) and response surface methodology (RSM) to evaluate the relationships between the independent variables and the response. These relationships were described using a second-order polynomial Equation 2:

$$Y = \beta_0 + \sum_{i=1}^{k} \beta_i X_i + \sum_{i=1}^{k} \beta_{ii} X_i^2 + \sum_{i=1}^{k} \sum_{j=i+1}^{k} \beta_{ij} X_i X_j \qquad (2)$$

RESULT AND DISCUSSION

Effect of SRE on boehmite synthesis

The successful synthesis of boehmite was confirmed both in the presence and absence of SRE, as evidenced by XRD analysis of the crystal structure of commercial γ-AlOOH and synthesized γ-AlOOH assisted by SRE extract. The presence of characteristic diffraction peaks further confirmed the formation of γ-AlOOH. The observed diffraction peaks at 2θ = 14.5°, 28.2°, 38.3°, 49°, 55.4°, 65°, 72°, and 86° were indicative of boehmite with an orthorhombic crystal structure. These peaks corresponded to entry code 96-901-2274 in the Crystallography Open Database.

The structural evolution of boehmite was strongly influenced by the concentration of SRE used during synthesis, as reflected in the crystallite size, interplanar spacing (d-spacing), and degree of crystallinity. The crystallite size of γ-AlOOH was calculated using the Scherrer equation. The presence of SRE affected crystal growth during the crystallization process. Slight variations in crystallite size were observed at SRE concentrations of 10% and 20%, while a significant decrease occurred at a higher concentration (50%).

This behavior is attributed to the role of SRE as a natural surfactant containing saponins with amphiphilic functional groups. Surfactants adsorb onto specific crystallographic planes, enhancing nucleation rates while inhibiting anisotropic crystal growth. As a result, the growth of individual crystallites is limited, leading to smaller crystallite sizes due to the formation of a larger number of nuclei. This observation is consistent with the findings of Zhu et al. (2004), who reported that

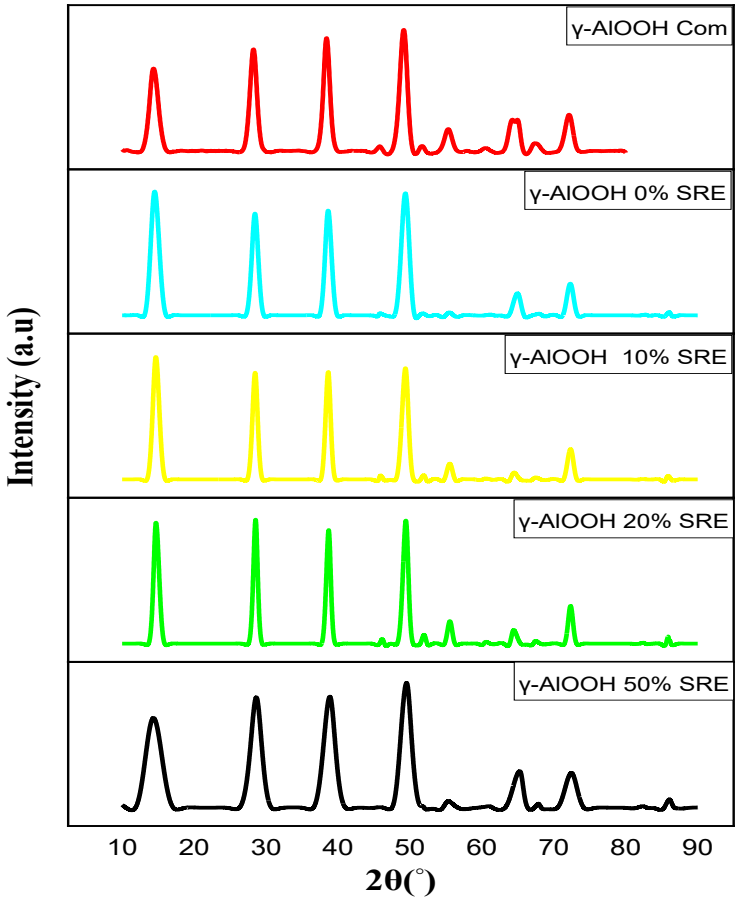

Figure 1. XRD pattern of (a) γ-AlOOH commercial, (b) γ-AlOOH 0% SRE, (c) γ-AlOOH 10% SRE, (d) γ-AlOOH 20% SRE, (e) γ-AlOOH 50% SRE.

surfactant micelles can regulate the growth of boehmite nanofibers. These micelles interact with the boehmite surface via hydrogen bonding involving hydroxyl groups, thereby directing crystal growth. The d-spacing values increased with increasing SRE concentration, suggesting the presence of lattice strain and structural distortion within the γ-AlOOH framework.

Boehmite has a layered orthorhombic structure composed of AlO_6 octahedra, with adjacent layers connected by hydrogen bonds. During the hydrothermal process, surface hydroxyl groups of γ-AlOOH can interact with hydroxyl and glycoside groups from SRE. This interaction disrupts interlayer hydrogen bonding, leading to expansion of the interlayer distance (Boumaza et al., 2009). Furthermore, crystallinity increased with higher SRE concentrations, likely due to more uniform nucleation, which promoted a more homogeneous crystal structure and reduced structural defects. These results align with the requirements for boehmite as a catalyst support, where high crystallinity and structural stability are essential (Handoko & Triyono 2023).

Boehmite functional group analysis

Figure 2 illustrates the FTIR spectra of boehmite synthesized with varying concentrations of SRE as a templating agent. The characteristic absorption bands of boehmite (γ-AlOOH) are clearly observed in the spectra. The band at 3288 cm^{-1} corresponds to asymmetric ν(Al–O–H) stretching vibrations of the hydroxyl groups, while the band at 3027 cm^{-1} is attributed to symmetric ν (Al–O–H) stretching vibrations, arising from hydrogen bonding between AlO_6 octahedral layers. The band at 1640 cm^{-1} is assigned to δ(H–O–H) bending vibrations, indicating the presence of water molecules adsorbed on the boehmite surface. The bands at 1160 cm^{-1} and 1068 cm^{-1} correspond to Al–O–H bending and combined hydroxyl deformation modes, which are characteristic of the

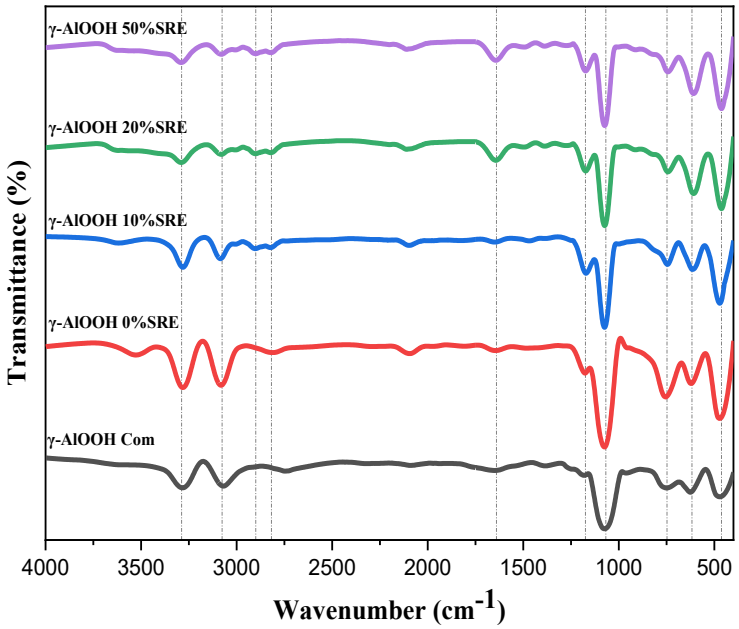

Figure 2. FTIR spectra of (a) γ-AlOOH commercial, (b) γ-AlOOH 0% SRE, (c) γ-AlOOH 10% SRE, (d) γ-AlOOH 20% SRE, (e) γ-AlOOH 50% SRE.

boehmite crystal structure. Furthermore, the bands at 746 cm^{-1}, 618 cm^{-1}, and 463 cm^{-1} are attributed to internal modes and Al–O lattice vibrations of AlO_6 octahedra (Van Truong & Kim 2022). Additional peaks observed at 1900 cm^{-1} and 2812 cm^{-1} in γ-AlOOH samples with 10%, 20%, and 50% SRE correspond to asymmetric CH_2 stretching and symmetric CH_2/CH_3 stretching vibrations, respectively. These peaks are not intrinsic to γ-AlOOH but are attributed to residual organic components from SRE (saponins), which contain long hydrocarbon chains (Nadhifah et al., 2025).

N_2 adsorption–desorption

Figure 3 illustrates a type IV isotherm with an H3 hysteresis loop for boehmite materials synthesized using varying concentrations of SRE (10%, 20%, and 50%) as a templating agent and Lapindo clay as the alumina source. The obtained N_2 adsorption–desorption isotherm follows the IUPAC classification, which is consistent with mesoporous materials (2–50 nm), as indicated by the type IV profile. The adsorption behavior in mesopores is governed by interactions between the adsorbent and adsorbate, as well as intermolecular interactions in the condensed phase. Initially, monolayer–multilayer adsorption occurs on the mesopore walls, followed by capillary condensation within the pores. The presence of an H3 hysteresis loop suggests slit-shaped pores, likely resulting from the use of SRE as a natural templating agent, which contributes to an irregular pore structure. The relatively narrow hysteresis loop in the P/P_0 range of 0.6–1.0 indicates significant capillary condensation. Such pore characteristics facilitate the diffusion of large hydrocarbon molecules, which would otherwise be hindered in smaller, narrower pores (Lv et al., 2023).

Table 2 shows that the surface area increases with increasing SRE (saponin) concentration, indicating that SRE functions as a structure-directing agent (SDA) in the synthesized boehmite. Meanwhile, the pore volume remains relatively constant as the SRE concentration increases. The observed decrease in pore diameter with higher SRE concentration suggests that SRE acts as a flexible template, promoting the formation of smaller and more abundant mesopores. These findings are consistent with the crystallite size obtained from XRD analysis, where smaller crystallite sizes correspond to larger surface areas and smaller pore diameters. The structural enhancement of boehmite through SRE is

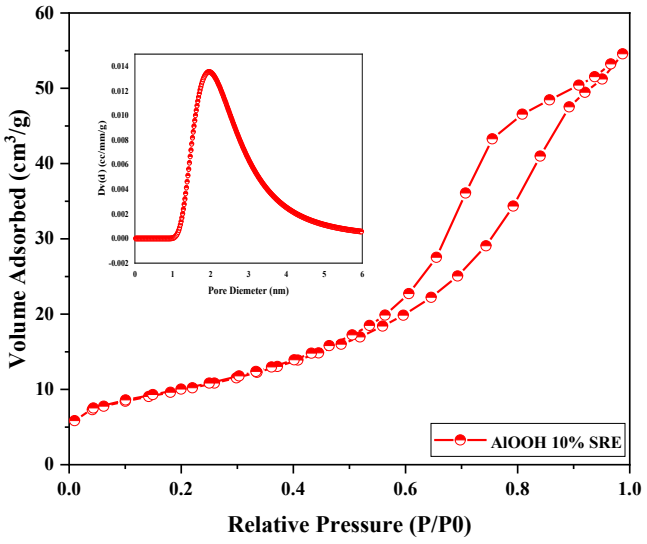

(a)

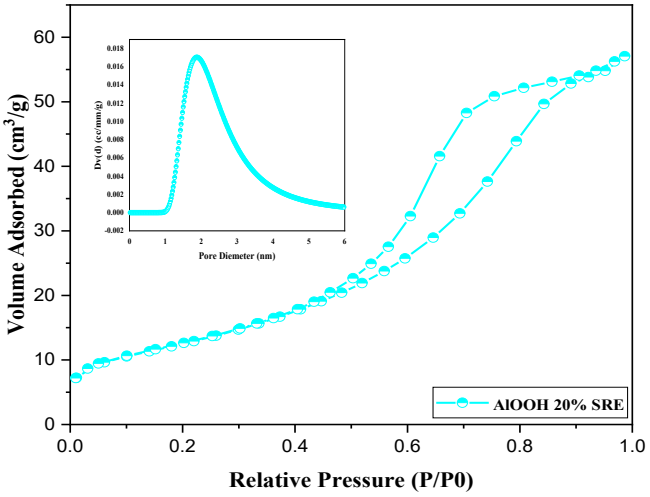

(b)

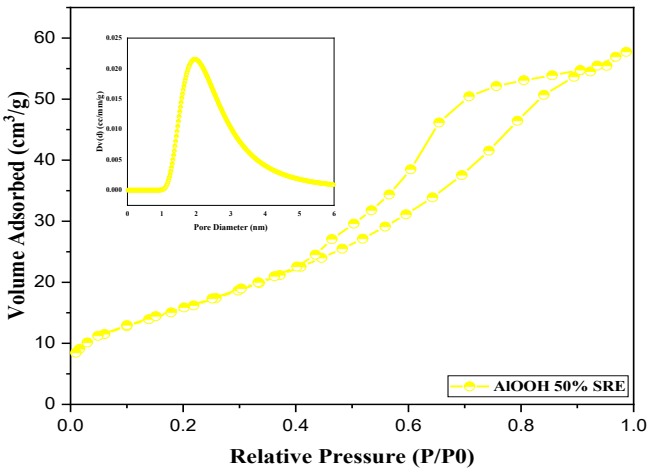

(c)

Figure 3. N_2 Adsorption-desorption Isotherms and pore size distribution of (a) γ-AlOOH 10% SRE, (b) γ-AlOOH 20% SRE, and (c) γ-AlOOH 50% SRE .

associated with the self-assembly of saponin micelles, which regulate nucleation and suppress excessive crystal growth during synthesis.

Statistical analysis of WCO deoxygenation

The experimental model employing the BBD method was used to investigate the impact of process parameters on the performance of boehmite as a catalyst in the deoxygenation of WCO into biofuel. The use of BBD enhanced the response surface estimation, as it ensures consistent spacing between factor levels throughout the design space (Goh et al., 2024). The experimental design based on BBD is presented in Table 2. The boehmite catalyst was tested under a reaction time of 4 hours, a temperature of 350°C, and a catalyst mass of 5 wt%. Under these conditions, the highest yield of 78.37% was obtained. A quadratic regression model was applied to analyze the BBD results and to characterize the relationship between the dependent and independent variables. The quadratic regression Equation 3 is expressed as follows:

$$Y = -1270.9 - 4.623\,X_1 + 22.648X_2 + 7.453X_3 + 0.973X_1X_2 + 0.001\,X_1X_3 - 0.054\,X_2X_3 + 0.404\,X_1^2 - 1.073\,X_2^2 - 0.01\,X_3^2 \quad (3)$$

The experimental variables significantly influence the conversion of WCO into biofuel, as indicated by the coefficients in the quadratic polynomial equation. A positive coefficient indicates a synergistic effect, whereas a negative coefficient indicates an antagonistic effect. Based on the magnitude of the coefficients, the conversion of WCO into biofuel using the γ-AlOOH 50% SRE catalyst is strongly influenced by parameters X_2 and X_3, as well as the interaction terms X_1X_2 and X_1X_3, and the quadratic term X_2^2. In contrast, parameters X_1, X_2X_3, X_1^2, and X_3^2 show a less significant influence on the conversion.

The adequacy of the mathematical model and the significance of each regression coefficient were evaluated using ANOVA, as presented in Table 3. The significance of variables in the WCO deoxygenation process using γ-AlOOH 50% SRE is determined by the F-value and p-value. A p-value less than 0.05 indicates statistical significance. The sign of each coefficient (±) reflects the effect of increasing or decreasing the corresponding parameter on the reaction outcome. The ANOVA results demonstrate that the model has a significant effect in predicting the deoxygenation performance of WCO using the γ-AlOOH 50% SRE catalyst, as indicated by a p-value < 0.05. The quadratic model adequately represents the experimental data within the studied range, as the lack-of-fit p-value is not significant (> 0.05). Table 4 further illustrates the model's

Table 1. Crystallite size, crystallinity, and d-spacing of γ-AlOOH.

Sample (γ-AlOOH)	Crystallite Size (nm)	Crystallinity (%)	d-spacing (Å)
Comm.	6.47	90.20	2.368
0% SRE	13.88	80.03	2.353
10% SRE	12.34	81.51	2.357
20% SRE	10.61	83.54	2.465
50% SRE	7.09	97.28	2.557

Table 2. Physicochemical properties of SRE-Supported γ-AlOOH catalyst.

Sample	Surface area (m^2/g)			Pore volume (cm^3/g)			Pore diameter (nm)
	S_{BET}	S_{meso}	S_{micro}	V_{Total}	V_{meso}	V_{micro}	
γ-AlOOH 10%SRE	54.93	36.13	35.82	0.0846	0.0801	-	9.4501
γ-AlOOH 20%SRE	66.30	44.93	45.32	0.0885	0.0846	-	7.8074
γ-AlOOH 50%SRE	85.72	51.25	57.97	0.0895	0.084	-	6.1785

effectiveness in predicting WCO conversion into biofuel. The coefficient of determination (R^2 = 0.8741) indicates that the model explains more than 87.4% of the variability in the experimental data. Additionally, the difference between the adjusted R^2 and predicted R^2 is less than 0.2, confirming the model's reliability in correlating process parameters with deoxygenation performance. The adequate precision value (10.6146) indicates a strong signal-to-noise ratio, demonstrating that the model provides reliable predictions (Sebayang et al., 2023).

The 3D response surface and contour plots in Figure 4 generally show that increases in reaction time, temperature, and catalyst mass lead to higher yields of WCO deoxygenation products. The more intense red regions indicate the optimal process conditions, while the blue regions represent minimal product yield. The curvature of the 3D response surface suggests significant interactions among the parameters as well as a pronounced quadratic effect. Figure 4(a) illustrates the relationship between catalyst mass and temperature, indicating high yields at catalyst masses exceeding 3.5% (w/w) within a temperature range of 335°C to 370°C. Figure 4(b) presents the relationship between catalyst mass and reaction time, showing that optimal conditions are achieved at reaction times of 2 to 4 hours and catalyst masses between 3.5% and 5% (w/w). The primary factors influencing WCO deoxygenation efficiency in biofuel production are reaction time and temperature, as illustrated in Figure 4(c), where the contour region appears relatively narrow. Optimal conditions are observed at reaction times exceeding 2 hours and temperatures ranging from 340°C to 370°C. Prolonged reaction times may promote over -cracking and hydrocarbon polymerization, while temperatures beyond this range can induce secondary cracking reactions (Jeon et al., 2024). Catalyst masses below 3.5% (w/w) provide fewer active sites, reducing the probability of simultaneous reactant adsorption and consequently prolonging the deoxygenation process (Goh et al., 2024).

Proposed reaction mechanism

The primary fatty acid profile in the WCO utilized in this investigation consists mainly of C16 and C18 chains, which are characteristic of palm oil (Lin et al., 2023). The final hydrocarbon chain distribution is largely determined by palmitic acid (C16:0), oleic acid (C18:1), linoleic acid (C18:2), and stearic acid (C18:0), which undergo decarboxylation, hydrodeoxygenation, and decarbonylation pathways. γ-AlOOH, arranged in an octahedral configuration, consists of layered structures interconnected by hydrogen bonding. The adsorption mechanism of fatty acid molecules is strongly influenced by the hydroxyl groups present on the γ-AlOOH surface, which facilitate the formation of bidentate or monodentate carboxylate species at Lewis acidic Al^{3+} sites. Following the wetness impregnation method and subsequent calcination in an N_2 atmosphere, the catalyst develops bifunctional active sites consisting of dispersed NiO species and the intrinsic acid–base sites of the boehmite structure.

These NiO species facilitate the deoxygenation of triglycerides under a non-hydrogen environment by promoting decarboxylation and decarbonylation pathways. The role of γ-AlOOH acidity is supported by the prevalence of surface hydroxyl groups and Al–O–H bending modes observed in FTIR analysis, which are characteristic of acid sites necessary for C–C bond cleavage (Gousi et al., 2017). The deoxygenation products of WCO using the γ-AlOOH 50% SRE catalyst are illustrated in Figure 6. Hydrocarbon chains in the range of C16–C21, indicative of green diesel, dominate the product distribution.

Figure 6 illustrates the proposed reaction mechanism. In the absence of excess hydrogen, triglycerides undergo β-elimination reactions at elevated temperatures, producing free fatty acids and glycerol fragments. Free fatty acids, including C16:0, C18:1, C18:2, and C18:0, are subsequently adsorbed onto the active sites of γ-AlOOH. The deoxygenation products consist of alkanes with carbon numbers equal to, one carbon less than, or greater than those of the parent fatty acids. This indicates the presence of multiple reaction pathways during WCO deoxygenation. The hydrodeoxygenation pathway involves the hydrogenation of the carboxyl group (R–COOH) to aldehydes, primary alcohols, and ultimately alkanes through the removal of H_2O, as evidenced by the formation of hexadecane (n-C16).

Table 3. Experimental model for the deoxygenation of WCO to biofuel using γ-AlOOH catalyst.

Run	Catalyst mass (% w/w)	Reaction time (h)	Temperature (°C)	Deoxygenation (%)	Predicted yield (%)
1	5	2.5	370	72.97	73.12
2	3	2.5	350	75.57	72.61
3	5	4	350	78.37	78.11
4	1	2.5	330	67.3	67.16
5	3	2.5	350	70.5	72.61
6	3	2.5	350	73.71	72.61
7	3	2.5	350	69.05	72.61
8	1	1	350	71.09	71.35
9	3	1	370	68.04	67.27
10	3	4	370	68.19	68.30
11	5	2.5	330	70.09	69.58
12	5	1	350	67.39	68.02
13	1	4	350	70.39	69.76
14	3	2.5	350	74.22	72.61
15	3	4	330	67.3	68.07
16	3	1	330	60.71	60.60
17	1	2.5	370	70	70.51

Table 4. P-values and F-values from BBD optimization.

Source	Sum of squares	Mean square	F-value	p-value
Model	224.98	25.00	5.40	0.0184 Significant
A – Catalyst Mass	12.60	12.60	2.72	0.1429
B – Reaction Time	36.21	36.21	7.82	0.0266
C – Temperature	23.81	23.81	5.14	0.0577
AB	34.11	34.11	7.37	0.0300
AC	0.0081	0.0081	0.0017	0.9678
BC	10.37	10.37	2.24	0.1781
A^2	10.98	10.98	2.37	0.1674
B^2	24.56	24.56	5.31	0.0547
C^2	71.99	71.99	15.55	0.0056
Residual	32.40	4.63		
Lack of Fit	2.71	0.9038	0.1218	0.9425 Not significant

Table 5. ANOVA results for deoxygenation performance.

Analysis	Deoxygenation performance	Analysis	Deoxygenation performance
Std. Dev.	2.15	Adjusted R^2	0.7123
Mean	70.29	Predicted R^2	0.6512
C.V. (%)	3.06	Adeq. Precision	10.6146
R^2	0.8741		

Decarboxylation proceeds via the formation of carboxylate intermediates at Al^{3+} sites, followed by C–C bond cleavage and the release of CO_2. In contrast, decarbonylation results in the formation of CO and H_2O. These pathways are evidenced by the formation of pentadecane (n-C15) and heptadecane (n-C17). The formation of hydrocarbons with longer carbon chains than the original fatty acids, such as eicosane (n-C20) and nonadecane (n-C19), suggests the occurrence of a ketonization mechanism. In this pathway, two fatty acid molecules combine to form a larger ketone intermediate, which is subsequently converted into long-chain hydrocarbons. The γ-AlOOH catalyst effectively facilitates ketonization due to the abundance of surface hydroxyl groups. Additionally, isomerization reactions occur at the acid sites of the γ-AlOOH catalyst. This process involves the formation of secondary carbocations along the alkane chain, followed by methyl shifts that produce more thermodynamically stable branched hydrocarbons. Such isomerization is beneficial for improving fuel properties, particularly cold-flow performance. Overall, the deoxygenation of WCO using the γ-AlOOH 50% SRE catalyst produces valuable hydrocarbon compounds comparable to green diesel (Yaghi et al., 2025).

CONCLUSION

The hydrothermal method was successfully employed to synthesize mesoporous boehmite, with SRE serving as a natural soft-template agent. The structure and crystal growth of boehmite were significantly influenced by the saponin content in SRE. An increase in SRE concentration resulted in a larger catalyst surface area, higher crystallinity, and smaller crystallite size. The sample prepared with 50% SRE exhibited the most favorable physicochemical characteristics, with a surface area of 85.72 m^2/g and a well-developed mesoporous structure. RSM optimization using the Box–Behnken Design demonstrated that temperature

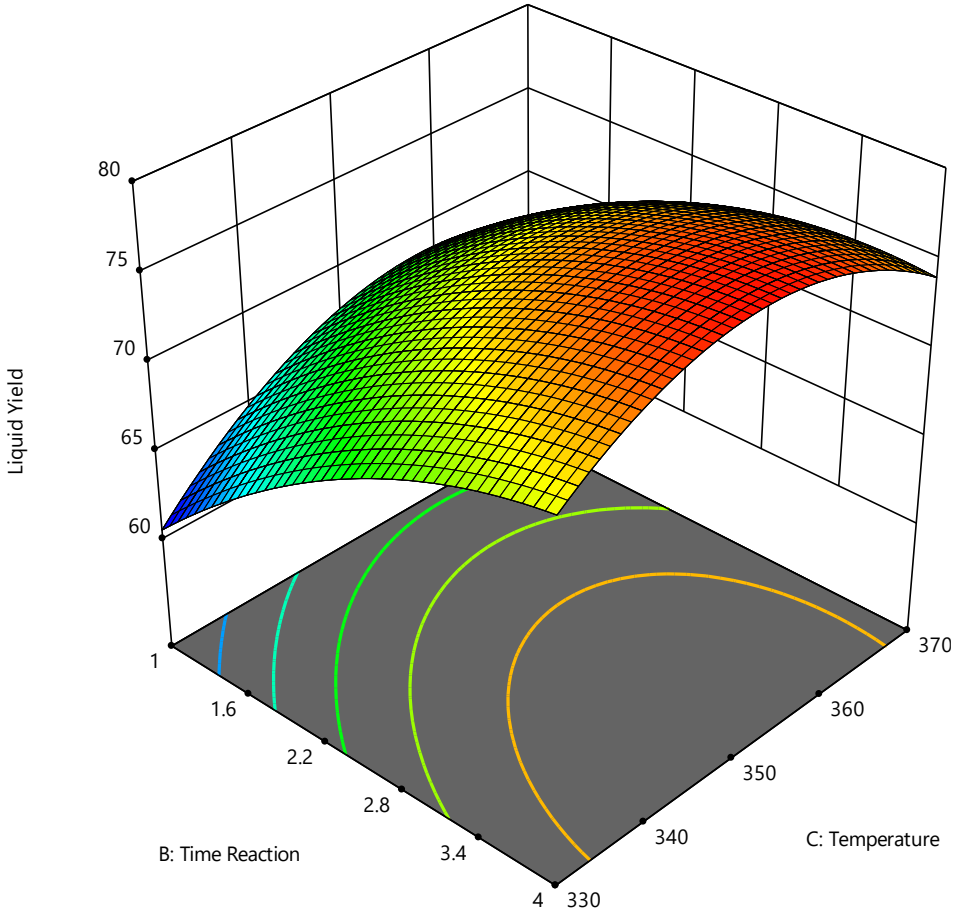

(a)

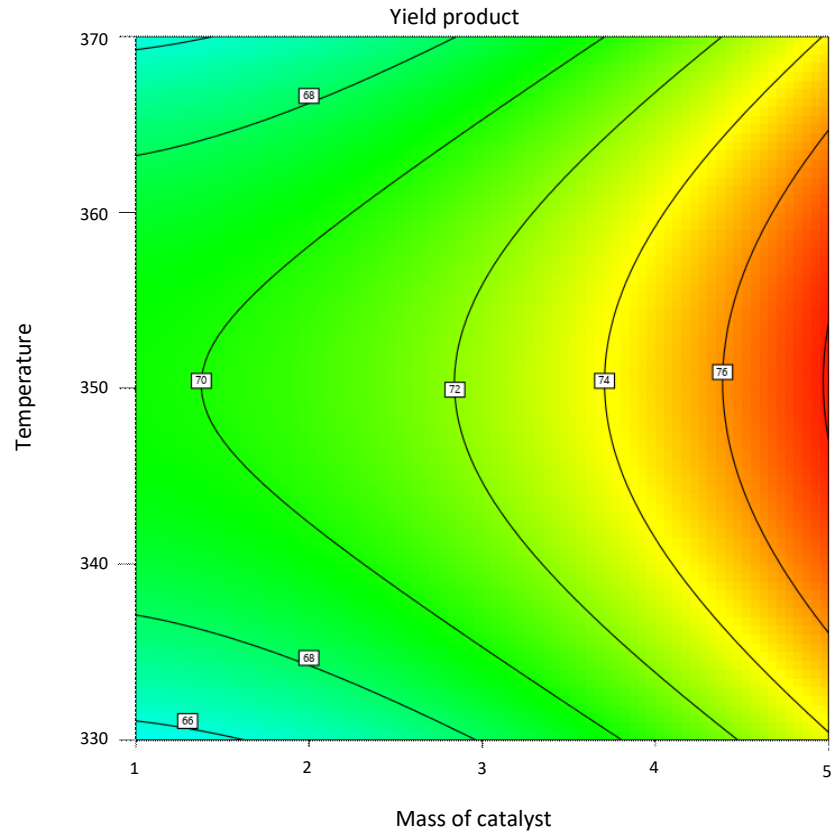
Yield product
Temperature
370
360
350
340
330
68
70
72
74
76
66
1
2
3
4
5
Mass of catalyst

(b)

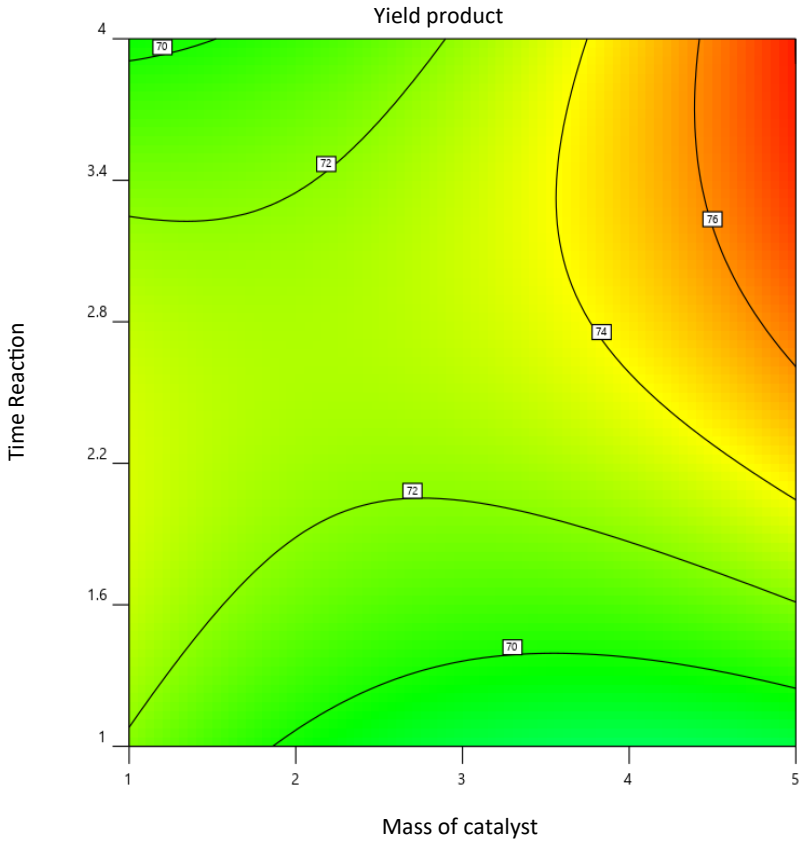
Yield product
Time Reaction
4
3.4
2.8
2.2
1.6
1
70
72
74
76
1
2
3
4
5
Mass of catalyst

(c)

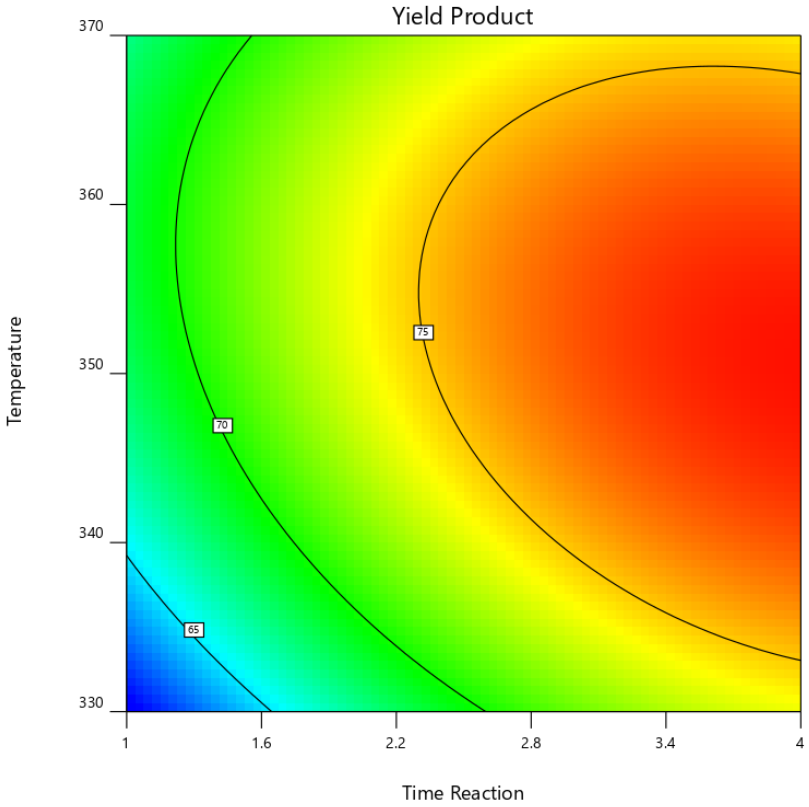

(d)

Figure 4. (a). 3D Surface plot; Contour plot interaction of (b). Mass catalyst and temperature, (c). Mass catalyst and time reaction, and (d) time reaction and temperature of optimum parameters

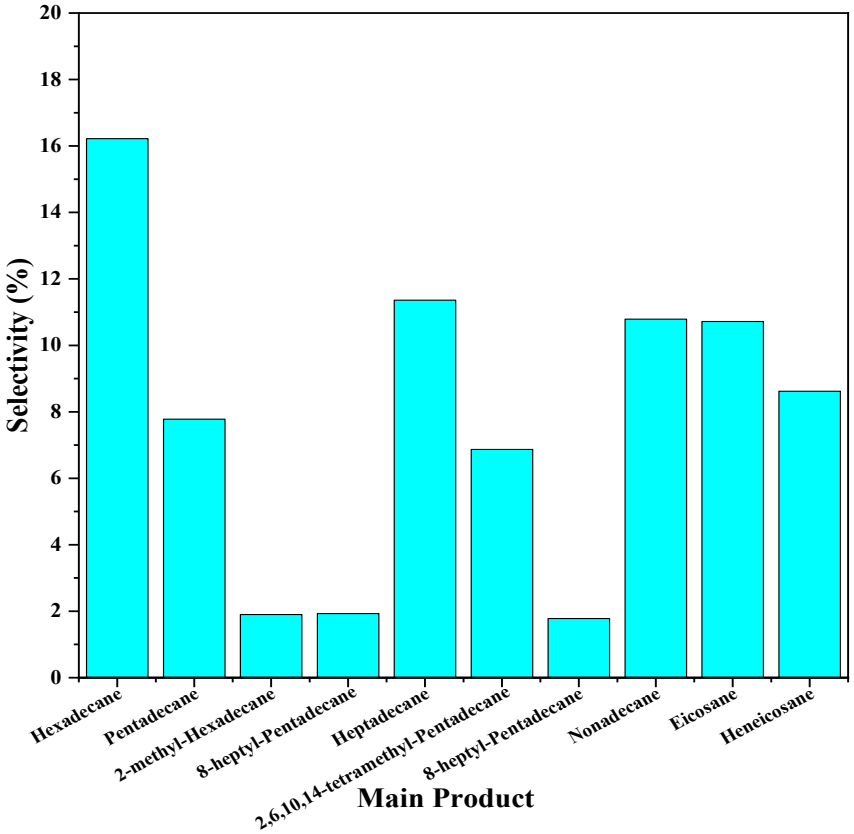

Figure 5. Composition of the main liquid fuel product from the WCO deoxygenation process using a 50% SRE γ-AlOOH catalyst.

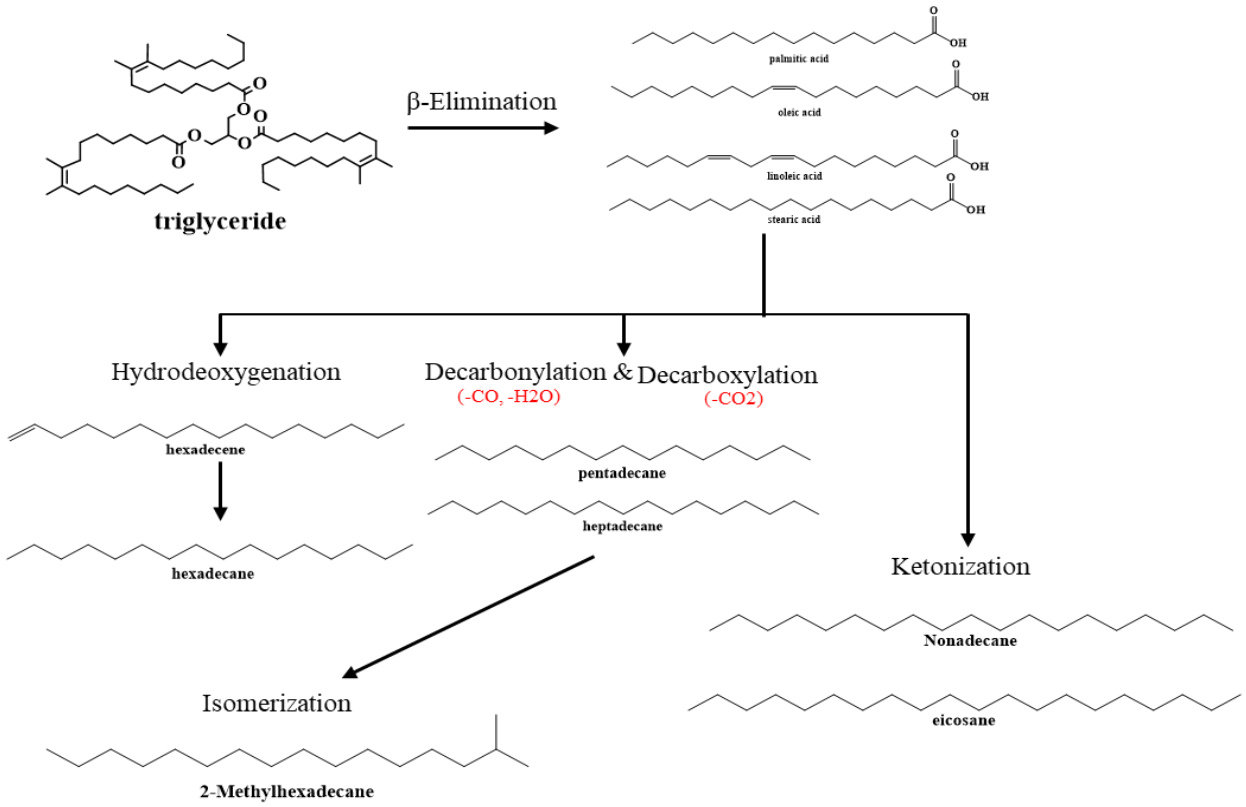

Figure 6. Proposed reaction mechanism for the deoxygenation of WCO into liquid fuel using a 50% SRE γ-AlOOH catalyst.

and reaction time were the most significant parameters influencing the WCO deoxygenation process. The optimal conditions were achieved at a catalyst loading of 5 wt%, a reaction temperature of 350°C, and a reaction time of 4 hours. Hydrocarbons in the C15–C21 range, corresponding to the diesel fraction, were identified as the predominant components in the deoxygenation products. These findings indicate that WCO conversion into diesel-range biofuel proceeds via deoxygenation pathways, including decarbonylation, decarboxylation, and hydrodeoxygenation. Overall, this study highlights the potential of natural templating agents and the development of sustainable catalysts for renewable fuel production from WCO.

ACKNOWLEDGEMENT

The authors gratefully acknowledge the National Research and Innovation Agency (BRIN) for funding this research through the Indonesia Advanced Research and Innovation (RIIM) scheme under contract number 330-04/ UN7.D2/KS/V/2023.

DECLARATIONS

Author contribution

Didi Dwi Anggoro: Writing – review & editing, Supervision, Investigation, Validation, Funding acquisition, Conceptualization. Luqman Buchori: Writing – review, Supervision, Investigation, Conceptualization. M. Hasim Muzadi: Writing – original draft, Methodology, Formal analysis, Data curation. Brilliant Umara Le Monde: Writing – review & editing, Methodology, Validation, Conceptualization. Tubagus Rayyan Fitra Sinuhaji: Writing – review & editing, Validation, Conceptualization. Sudiyarmanto: Writing – review & editing, Investigation, Validation, Conceptualization. Wawan Rustyawan: Writing – review & editing, Investigation, Validation, Conceptualization.

Funding statement

None

Competing interest

None

The use of AI or AI-assisted technologies

None

GLOSSARY OF TERMS AND SYMBOLS

Terms & Symbols	Definition	Unit
WCO	Waste cooking oil	-
SRE	Sapindus rarak Extract	-
γ-AlOOH	Boehmite	-
X_1	Catalyst mass	wt%
X_2	Reaction time	H
X_3	Temperature	°C
Y	Product yield	%
RSM	Response surface methodology	-
BBD	Box–behnken design	-
S_{BET}	Specific surface area (BET method)	m^2/g
S_{Meso}	Mesopore surface area	m^2/g
S_{Mikro}	Micropore surface area	m^2/g
V_{Total}	Total pore volume	cm^3/g
V_{meso}	Mesopore volume	cm^3/g
k	Number of independent variables	-
β_i	Linear coefficient	-
β_{ii}	Quadratic coefficient	-
R^2	Coefficient of determination	-

REFERENCES

Abdollahifar, M., Hidaryan, M., & Jafari, P., (2018), The role anions on the synthesis of AlOOH nanoparticles using simple solvothermal method. Boletin de La Sociedad Espanola de Ceramica y Vidrio, 57(2), 66–72. https://doi.org/10.1016/j.bsecv.2017.06.002.

Ameri, E., Abdollahifar, M., Zamani, M. R., & Nekouei, H., (2016), The role of urea on the hydrothermal synthesis of boehmite nanoarchitectures. Ceramics - Silikaty, 60(2), 162–168. https://doi.org/10.13168/cs.2016.0025

Aziz, A., Andini Putri, B. G., Prasetyoko, D., Nugraha, R. E., Holilah, H., Bahruji, H., Jalil, A. A., Suprapto, S., Hartati, H., & Asikin-Mijan, N., (2023), Synthesis of mesoporous zeolite Y using Sapindus rarak extract as natural organic surfactant for deoxygenation of Reutealis trisperma oil to biofuel. RSC Advances, 13(46), 32648–32659. https://doi.org/10.1039/d3ra05390c.

Aziz, A., Nugraha, R. E., Holilah, H., Bahruji, H., Al Muttaqii, M., Suprapto, S., & Prasetyoko, D., (2024), Hydrothermal study of synthesis mesoporous NaP zeolite using Sapindus rarak extract as natural surfactant. Inorganic Chemistry Communications, 165(April). https://doi.org/10.1016/j.inoche.2024.112497.

Banks, S. W., & Bridgwater, A. V., (2016), Catalytic fast pyrolysis for improved liquid quality. In Handbook of Biofuels Production (pp. 391–429). Elsevier. https://doi.org/10.1016/B978-0-08-100455-5.00014-X.

Boumaza, A., Favaro, L., Lédion, J., Sattonnay, G., Brubach, J. B., Berthet, P., Huntz, A. M., Roy, P., & Tétot, R., (2009), Transition alumina phases induced by heat treatment of boehmite: An X-ray diffraction and infrared spectroscopy study. Journal of Solid State Chemistry, 182(5), 1171–1176. https://doi.org/10.1016/j.jssc.2009.02.006.

Dabbawala, A. A., Al Maksoud, W., Abou-Hamad, E., Charisiou, N. D., Constantinou, A., Harkou, E., Latsiou, A. I., AlKhoori, S., Hinder, S. J., Baker, M. A., Anjum, D. H., Kobayashi, Y., Goula, M. A., & Polychronopoulou, K., (2024), Tuning of the acid sites in the zeolite-alumina composite Ni catalysts and their impact on the palm oil hydrodeoxygenation reaction. Chemical Engineering Journal, 493, 152351. https://doi.org/10.1016/j.cej.2024.152351.

Dwi Anggoro, D., Buchori, L., . S., Rustyawan,

W., Shafira, R., & Umara Le Monde, B., (2024), Hydrothermal Synthesis of Well-Crystallized Boehmite from Lapindo Mud: Process Optimization. International Journal of Chemical and Biochemical Sciences, 25(19). https://doi.org/10.62877/80-IJCBS-24-25-19-80

Goh, B. H. H., Chong, C. T., Milano, J., Tiong, S. K., Cui, Y., & Ng, J.-H., (2024), Response optimisation of TiO2-supported bimetallic NiCo catalyst for the cracking and deoxygenation of waste cooking oil into jet-fuel range hydrocarbon fuels under non-hydrogen environment. Energy, 309, 133057. https://doi.org/10.1016/j.energy.2024.133057.

Gousi, M., Andriopoulou, C., Bourikas, K., Ladas, S., Sotiriou, M., Kordulis, C., & Lycourghiotis, A., (2017), Green diesel production over nickel-alumina co-precipitated catalysts. Applied Catalysis A: General, 536, 45–56. https://doi.org/10.1016/j.apcata.2017.02.010.

He, F., Li, W., Pang, T., Zhou, L., Wang, C., Liu, H., Li, M., & He, X., (2022), Hydrothermal synthesis of boehmite nanorods from alumina sols. Ceramics International, 48(13), 18035–18047. https://doi.org/10.1016/j.ceramint.2022.02.212.

Ibrahim, O. M., Habib, B. S., Alazemi, A. A., & Aljuwayhel, N. F., (2026), Synthesis and surface characterization of boehmite and activated alumina coatings on FeCrAl sintered fibers. Results in Surfaces and Interfaces, 22, 100675. https://doi.org/10.1016/j.rsurfi.2025.100675.

Jeon, K.-W., Gong, J.-H., Kim, M.-J., Shim, J.-O., Jang, W.-J., & Roh, H.-S., (2024), Review on the production of renewable biofuel: Solvent-free deoxygenation. Renewable and Sustainable Energy Reviews, 195, 114325. https://doi.org/10.1016/j.rser.2024.114325.

Jovita, S., Holilah, H., Khairunisa, N. N., Bahruji, H., Nugraha, R. E., Sholeha, N. A., Aziz, A., Ediati, R., Jalil, A. A., & Prasetyoko, D., (2024), Mesoporous silica catalyst using Sapindus rarak extract as template for deoxygenation of waste cooking oil to biofuels. Case Studies in Chemical and Environmental Engineering, 10(September). https://doi.org/10.1016/j.cscee.2024.100935.

Li, Y., Zhang, X., Shang, C., Wei, X., Wu, L., Wang, X., Wu, W. D., Chen, X. D., Selomulya, C., Zhao, D., & Wu, Z., (2020), Scalable Synthesis of Uniform Mesoporous Aluminosilicate Microspheres with Controllable Size and Morphology and High Hydrothermal Stability for Efficient Acid Catalysis. ACS Applied Materials & Interfaces, 12(19), 21922–21935. https://doi.org/10.1021/acsami.0c04998.

Lin, D., Mao, Z., Shang, J., Zhu, H., Liu, T., Wu, Y., Li, H. Z., Peng, C., & Feng, X., (2023), Catalyst Design Strategies for Deoxygenation of Vegetable Oils to Produce Second-Generation Biodiesel. Industrial & Engineering Chemistry Research, 62(32), 12462–12481. https://doi.org/10.1021/acs.iecr.3c01542.

Liu, H., Zhou, J., Li, G., Han, X., Li, T., Gao, X., Xie, F., Wan, P., & Liu, H., (2023), Synthesis of Mesoporous Aluminosilicates with Moderate Acidity and High Hydrothermal Stability by Acid-Free Method. Industrial & Engineering Chemistry Research, 62(47), 20251–20258. https://doi.org/10.1021/acs.iecr.3c02395.

Lv, M., Song, S., Verma, P., & Wen, M., (2023), Hollow mesoporous aluminosilicate spheres imbedded with Pd nanoparticles for high performance toluene combustion. Catalysis Today, 410, 135–142. https://doi.org/10.1016/j.cattod.2022.06.009.

Morina, M., & Sidjabat, O., (2022), Catalytic Pyrolysis Of Polypropylene Plastic From Municipal Solid Wastes Into Gasoline Fraction Compounds Using The Mixed Nickel (Ni) And Chrome (Cr) Metals As The Catalyst. Scientific Contributions Oil and Gas, 37(3), 129–140. https://doi.org/10.29017/SCOG.37.3.634.

Movasati, B., Aminian, F., & Norouzbeigi, R., (2024), Morphological synthesis of boehmite nanoparticles utilizing xanthan gum: A nature-based directing agent effect optimization. Results in Engineering, 24, 103585. https://doi.org/10.1016/j.rineng.2024.103585.

Nadhifah, N., Jovita, S., Subagyo, R., Utami, D. I., Agustina, K. R., Holilah, H., Asikin-Mijan, N., Bahruji, H., Nugraha, R. E., Jalil, A. A., Suprapto, S., & Prasetyoko, D., (2025), Mesoporous aluminosilicate from metakaolin with natural surfactants for waste cooking oil conversion to hydrocarbon fuels via low-temperature pyrolysis. Case Studies in Chemical and Environmental Engineering, 11, 101111. https://doi.org/10.1016/j.cscee.2025.101111.

Nasution, N., E. Jasjfi, E. J., & Morina, M., (2022), Proses Alkilasi dan Peranannya dalam Pembuatan Bahan Bakar Bensin Ramah Lingkungan. Lembaran Publikasi Minyak Dan Gas Bumi, 40(1), 25–32. https://doi.org/10.29017/LPMGB.40.1.178.

Nugraha, R. E., Prasetyoko, D., Asikin-Mijan, N., Bahruji, H., Suprapto, S., Taufiq-Yap, Y. H., & Jalil, A. A., (2021), The effect of structure directing agents on micro/mesopore structures of aluminosilicates from Indonesian kaolin as deoxygenation catalysts. Microporous and Mesoporous Materials, 315, 110917. https://doi.org/10.1016/j.micromeso.2021.110917.

Purwo Handoko, D. S., & Triyono, T., (2023), The Effect Of Acid Strength Of Bronsted Acid Site On The Ability Of The Catalyst To Break The Carbon Chain Bonds Of 1-Octadekenes Into Alkanes And Short Chain Alkenes As A Substitute For Fossil Fuels. Scientific Contributions Oil and Gas, 46(1), 1–7. https://doi.org/10.29017/SCOG.46.1.1311.

Sebayang, A. H., Ideris, F., Silitonga, A. S., Shamsuddin, A. H., Zamri, M. F. M. A., Pulungan, M. A., Siahaan, S., Alfansury, M., Kusumo, F., & Milano, J., (2023), Optimization of ultrasound-assisted oil extraction from Carica candamarcensis; A potential Oleaginous tropical seed oil for biodiesel production. Renewable Energy, 211, 434–444. https://doi.org/10.1016/j.renene.2023.04.099.

Setyawan, D., Yono, T., & Rina, M., (2018), Aktivitas Katalis Ni/Zeolit pada Konversi Katalitik Metil Ester Minyak Goreng Jelantah (Mewco) pada Temperatur 450OC Menjadi Senyawa Fraksi Bahan Bakar. Lembaran Publikasi Minyak Dan Gas Bumi, 43(1), 65–74. https://doi.org/10.29017/LPMGB.43.1.129.

Spiegel, S., (2018), Polymer/Boehmite Nanocomposites: A Review. Journal of Applied Polymer Science, 135(24). https://doi.org/10.1002/app.46279.

Sun, Y., Shi, Z., Wang, J., & Xu, K., (2025), Preparation of Boehmite by the Hydrothermal Method and Analysis of its Dehydration Kinetics. Powder Metallurgy and Metal Ceramics, 63(11–12), 712–721. https://doi.org/10.1007/s11106-025-00497-x.

Toledo-Chávez, G., Paniagua-Rodríguez, J.-C., Zárate-Medina, J., & Maya-Yescas, R., (2016), Reactions analysis during the synthesis of pseudo-boehmite as precursor of gamma-alumina. Catalysis Today, 271, 207–212. https://doi.org/10.1016/j.cattod.2015.07.056.

Ulfiati, R., (2020), Catalytic Performance Of Zsm-5 Zeolite In Heavy Hydrocarbon Catalytic Cracking: A Review. Scientific Contributions Oil and Gas, 42(1), 29–34. https://doi.org/10.29017/SCOG.42.1.384.

Van Truong, T., & Kim, D.-J., (2022), Synthesis of high quality boehmite and γ-alumina for phosphorus removal from water works sludge by extraction and hydrothermal treatment. Environmental Research, 212, 113448. https://doi.org/10.1016/j.envres.2022.113448.

Yaghi, M., Chidiac, S., Awad, S., El Rayess, Y., & Zgheib, N., (2025), An Overview of Biodiesel Production via Heterogeneous Catalysts: Synthesis, Current Advances, and Challenges. Clean Technologies, 7(3), 62. https://doi.org/10.3390/cleantechnol7030062.

Yang, Y., Xu, X., He, H., Huo, D., Li, X., Dai, L., & Si, C., (2023), The catalytic hydrodeoxygenation of bio-oil for upgradation from lignocellulosic biomass. International Journal of Biological Macromolecules, 242, 124773. https://doi.org/10.1016/j.ijbiomac.2023.124773.

Zhu, H. Y., Gao, X. P., Song, D. Y., Bai, Y. Q., Ringer, S. P., Gao, Z., Xi, Y. X., Martens, W., Riches, J. D., & Frost, R. L., (2004), Growth of

Boehmite Nanofibers by Assembling Nanoparticles with Surfactant Micelles. The Journal of Physical Chemistry B, 108(14), 4245 –4247. https://doi.org/10.1021/jp049485u.